Available online at www.sciencedirect.com

ScienceDirect

Procedia Materials Science 8 (2015) 11 – 20

Procedia Materials Science

www.elsevier.com/locate/procedia

International Congress of Science and Technology of Metallurgy and Materials, SAM - CONAMET 2013

Effect of Environmental Variables on Crevice Corrosion Susceptibility of Ni-Cr-Mo Alloys for Nuclear Repositories

Edgar C. Hornus[(a,b)],Martín A. Rodríguez[(a,b,c)], Ricardo M. Carranza[(a,b)],C. Mabel Giordano[(a,b)], Raúl B. Rebak[(d)]*

[(a)]*Instituto Sabato, UNSAM-CNEA, Av. Gral. Paz 1499,San Martín B1650KNA,Buenos Aires ,Argentina*
[(b)] *Gerencia Materiales, Centro Atómico Constituyentes, CNEA, Av. Gral. Paz 1499, San Martín, B1650KNA Buenos Aires, Argentina*
[(c)] *Consejo Nacional de Investigaciones Científicas y Técnicas, Argentina*
[(d)] *GE Global Research Schenectady, NY 12309, USA*

Abstract

The crevice corrosion repassivation potential was determined by the Potentiodynamic-Galvanostatic-Potentiodynamic (PD-GS-PD) method. Alloys 625, C-22, C-22HS and HYBRID-BC1 were used. Specimens contained 24 artificially creviced spots formed by a ceramic washer (crevice former) wrapped with a PTFE tape. Crevice corrosion tests were performed in 0.1 mol/L and 1 mol/L NaCl solutions at temperatures between 20 and 90ºC, and $CaCl_2$ 5 mol/L solution at temperatures between 20 and 117°C. The crevice corrosion resistance of the alloys increased in the following order: 625 < C-22 < C-22HS < HYBRID-BC1. The repassivation potential (E_{CO}) showed the following relationship with temperature (T) and chloride concentration ($[Cl^-]$) $E_{CO} = (a + b\ T) \log [Cl^-] + c\ T + d$; where a, b, c and d are constants. At temperatures above 90°C, E_{CO} for alloy 625 stabilized at a minimum value of -0.26 V_{SCE}.

Selection and peer-review under responsibility of the scientific committee of SAM - CONAMET 2013

Keywords: localized corrosion; repassivation potential; temperature; chloride

* Corresponding author. Tel.: +54-116-772-7353; fax: +54-116-772-7362.
E-mail address: hornus@cnea.gov.ar

Selection and peer-review under responsibility of the scientific committee of SAM - CONAMET 2013
doi:10.1016/j.mspro.2015.04.043

1. Introduction

Deep geological disposal is the strongest alternative to the disposal of high level nuclear waste (Whiterspoon and Bodvarsson, 2001). Geological repositories are based on the multi-barrier principle, which consists in interposing a number of natural and engineering barriers between waste and the biosphere. The waste containers are the main engineering barrier. Due to its excellent resistance to general and localized corrosion, nickel alloys are among the considered materials for the fabrication of the outer shell of the high level nuclear waste containers (Gras, 2002). The containers are designed to isolate radioactive waste from the environment for periods of hundreds to thousands of years. For the construction of containers metallic materials are selected that meet the requirements of corrosion resistance, mechanical strength, good heat dissipation and stability against heat and radiation. Localized corrosion, like crevice or pitting corrosion, is one of the most important degradation processes that will limit the containers lifetime. The growth of a pit generates a morphology that is essentially a crevice, so active pits and crevices are basically identical. The phenomenological aspects of pitting apply equally to crevice corrosion. However, crevice corrosion is more likely, since it is stabilized in occluded regions at lower potentials than pitting corrosion (Szklarska-Smialowska, 2005; Combrade, 2000; Galvele and Duffó, 2006; Fontana, 1986). Crevices may occur due to the presence of deposits, corrosion products, etc. (Fontana, 1986). The crevice corrosion susceptibility of an alloy is measured by its repassivation potential (E_{CO}) (Rebak, 2000). The lower is E_{CO}, the more aggressive is the environment (Szklarska-Smialowska, 2005). The PREN (Pitting Resistance Equivalent Number) is frequently used as an indicative measure of the alloys resistance to localized corrosion. It was developed originally for stainless steel, and then adapted to nickel-base alloys (Combrade, 2000). PREN is defined in Equation 1 as a function of weight percentages of the alloying elements Cr, Mo and W (Szklarska-Smialowska, 2005). A recent work indicates that PREN is in agreement with the crevice corrosion resistance ranking of nickel alloys bearing chromium and molybdenum (Zadorozne et al., 2012).

$$PREN = \%Cr + 3.3(\%Mo + 0.5\%W) \quad (1)$$

Temperature and chloride concentration are among the key parameters in affecting the alloys susceptibility to localized attack. The waste containers will be under a heat dissipation determined by the waste heat through the repository (Whiterspoon and Bodvarsson, 2001). The temperature of the containers will increase reaching a peak due to the heat dissipation from the waste, surpassing even the boiling point of water. If this happens, the amount of moisture in contact with the containers would be limited. Then the temperature will slowly decrease (Yucca Mountain Science and Engineering Report, 2001). It has been shown that the temperature has a strong effect on crevice corrosion properties of nickel-based alloys. The environment in contact with the containers, initially hot dry-air, may become an aggressive aqueous solution as a result of dripping of groundwater and evaporative concentration due to radioactive decay heating (Whiterspoon and Bodvarsson, 2001; Gordon, 2002). The main aggressive ion present in groundwater is chloride (Cragnolino, 2001; MacDougall, 2001). The objective of this work was to assess the effects of temperature and chloride concentration on the crevice corrosion resistance of selected Ni-Cr-Mo alloys.

2. Experiment

The chemical composition of the alloys in weight percent are listed in Table 1.

The crevice corrosion repassivation potential was determined by the Potentiodynamic-Galvanostatic-Potentiodynamic (PD-GS-PD) method. This is a modification of the Tsujikawa-Hisamatsu Electrochemical (THE) method (ASTM G 192) (Evans et al., 2005; Mishra and Frankel, 2008; Rincón Ortíz et al., 2010). It consists of three stages:

- A potentiodynamic polarization in the anodic direction up to reaching an anodic current of 30-300 μA.
- Galvanostatic step. Application of this 30-300 μA for 2 hours.
- Potentiodynamic polarization in the cathodic direction, from the end potential of the previous setup to reaching alloy repassivation.

The scan rate was 0.167 mV/s. Before each PD-GS-PD test, the corrosion potential was monitored for 15 minutes. Then, a 5 μA galvanostatic cathodic pretreatment of 5 min was performed before the initiation of the anodic potential scan of step 1.

Multiple crevice assemblies (PCA) specimens were used in the crevice corrosion tests. They were fabricated based on ASTM G-48 that contained 24 artificially creviced spots formed by a ceramic washer (crevice former) wrapped with a PTFE tape (ASTM G 192-08). The total surface area of the PCA specimen immersed in the electrolyte was approximately 14 cm^2. The applied torque was 5 Nm. The specimens had a finished grinding of SiC abrasive paper number 600 and they were degreased in acetone and washed in distilled water. Tests were performed in duplicate or triplicate. The testing solutions were 0.1 mol/L NaCl, 1 mol/L NaCl and 5 mol/L $CaCl_2$. Tests were performed in the temperature range from 20ºC to 90ºC in 0.1 mol/L NaCl and 1 mol/L NaCl solutions, and from 20ºC to 117ºC in 5 mol/L $CaCl_2$ solutions (5 mol/L $CaCl_2$ boils at 120ºC). The higher solubility of $CaCl_2$, compared with that of NaCl, allowed the preparation of 10 mol/L chloride solutions.

Table 1.Chemical composition of the tested alloys in weight percent.

Alloy	Ni	Cr	Mo	W	Fe	Co	Si	Mn	C	V	Al	B	Cb+Ta
625	62	21	9	0	5	1	0.5	0.5	0.1	0	0.4	0	3.7
C-22	56	22	13	3	3	2.5	0.08	0.5	0.01	0.35	0	0	0
C-22HS	61	21	17	1	2	1	0.08	0.8	0.01	0	0.5	0.006	0
HYBRID-BC1	62	15	22	0	2	0	0.08	0.25	0.01	0	0.5	0	0

Electrochemical tests were conducted in a one-liter, three-electrode vessel. A water-cooled condenser combined with a water trap was used to avoid evaporation of the solution and to prevent the ingress of air (oxygen). The temperature of the solution was controlled by immersing the cell in a water bath, which was kept at a constant temperature. Nitrogen (N_2) was purged through the solution 1 hour prior to testing and it was continued throughout the entire test. The reference electrode was a saturated calomel electrode (SCE), which has a potential of 0.242 V more positive than the standard hydrogen electrode (SHE) at room temperature. The counter electrode consisted of a platinum wire (with a total area of 20 cm^2 approximately). All the potentials are reported in the SCE scale. Post-test analysis included examination in an optical stereomicroscope and scanning electron microscope (SEM).

3. Results and Discussion

3.1. Determination of the crevice corrosion repassivation potential (E_{CO})

Figure 1 shows the determination of the crevice corrosion repassivation potential of alloy C-22 in 5 mol/L $CaCl_2$ at 60ºC. The crevice corrosion repassivation potential for this technique is a cross-over repassivation potential determined at the intersection of the forward (stage 1) and reverse (stage 3) scans (Figure 1). Once the current density reached a predetermined value (30 μA or 2 μA/cm^2 in most of cases), the controlling mode was switched from potentiodynamic to galvanostatic and the predetermined current density was applied for 2 hours. This current was occasionally increased one order of magnitude for systems with higher passive current densities or with anodic current peaks in the passivity potential range. This current variation did not significantly affect the value of E_{CO} (Rincón Ortíz et al., 2010).

Figure 2 shows the morphology of the crevice corrosion attack of alloy C-22 tested in $CaCl_2$ 5 mol/L at 60°. The attack started at the crevice former/metal interface and progressed outward towards the non-occluded surface. Figure 2 shows that the attack appears as a shiny crystalline area, under the microscope or even under the naked eye. This attack seemed to progress through the higher energy planes of the crystal structure of the grains (Rebak, 2005). The morphology observed in Figure 2 is representative of what occurred at different temperatures in the four studied alloys when tested in $CaCl_2$ 5 mol/L.

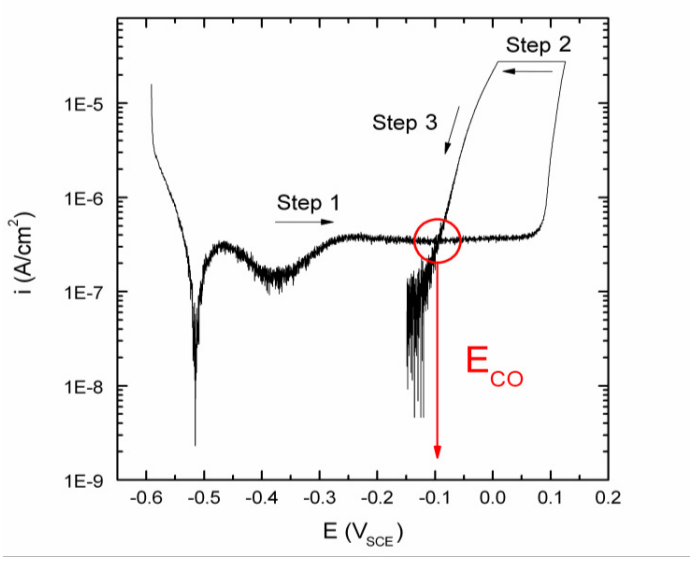

Fig. 1. PD-GS-PD technique used for determining crevice corrosion repassivation potential of alloy C-22 in 5 mol/L $CaCl_2$ at 60ºC.

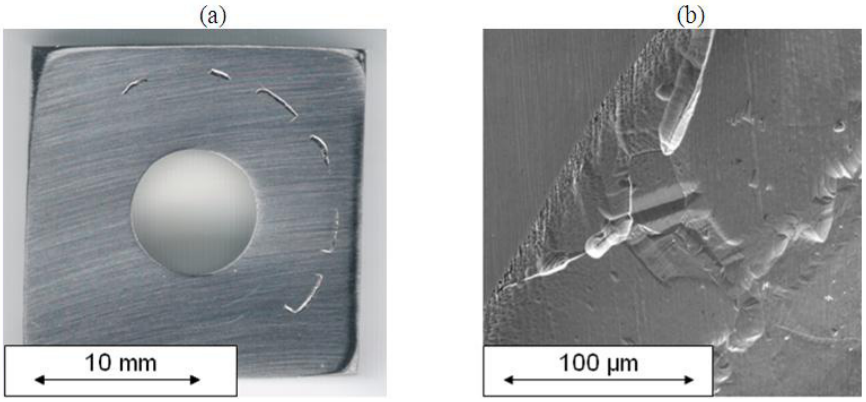

Fig. 2.Specimens of alloy C-22 in 5 mol/L $CaCl_2$, at 60ºC after a PD-GS-PD test. (a) Optical microscope image; (b) SEM image of the same specimen.

3.2. Effect of temperature and chloride concentration on E_{CO}

Figure 3 shows E_{CO} (average value and standard deviation) obtained using the PD-GS-PD method as a function of temperature (T) in chloride solutions of different concentration for the all the tested alloys. E_{CO} always decreased linearly with T except for alloy 625, where E_{CO} stabilized at -0.26 V_{SCE} for temperatures higher than 90°C, in 10 mol/L Cl^- solutions. No crevice corrosion was observed in alloy HYBRID-BC1 at low temperatures: below 70°C in 0.1 mol/L solutions Cl^-, and below 60°C in 1 and 10 mol/L Cl^- solutions. In the same way, no crevice corrosion was observed in alloy C-22HS at low temperatures: below 50°C in 1 and 10 mol/L Cl^- solutions, and below 40°C in 10 mol/L Cl^- solutions. Alloy C-22 suffered crevice corrosion only at T $\geqslant$ 40ºC for any chloride concentration. Alloy 625 suffered crevice corrosion in the entire studied temperature range, from 20 to 117ºC. No tests were

performed at temperatures below 20°C, thus a lower limit of temperature for crevice corrosion of alloy 625 could not be obtained.

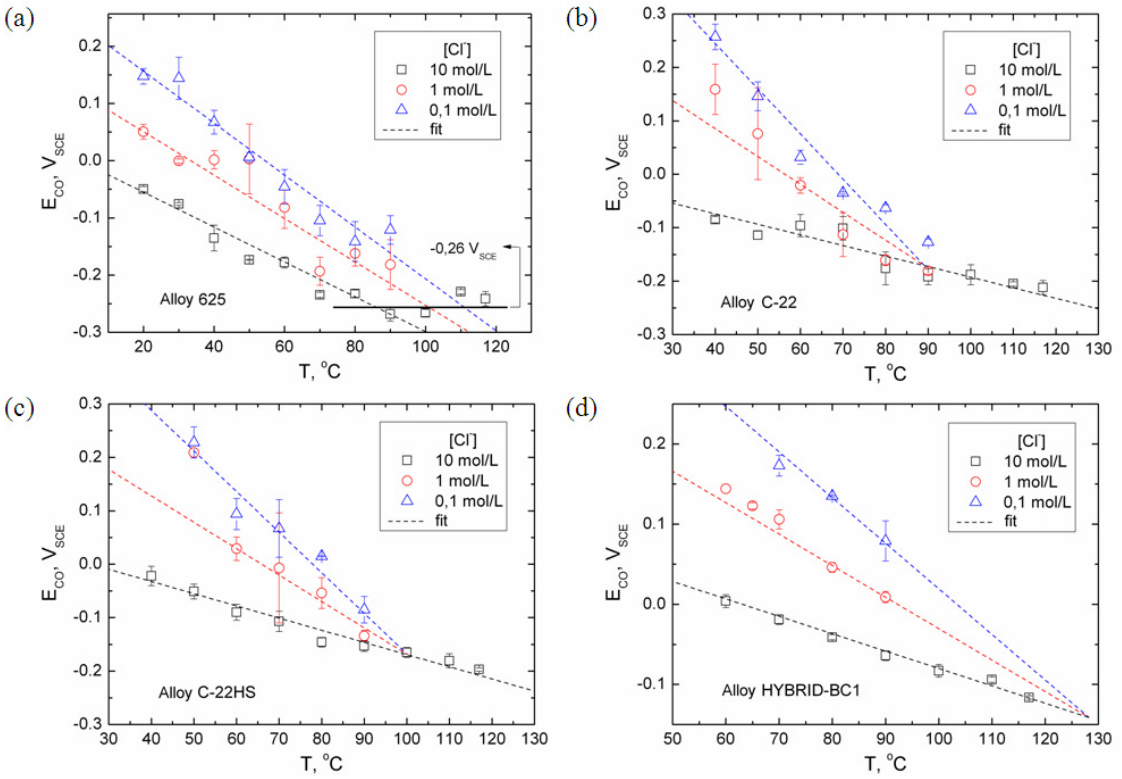

Fig. 3.E_{CO}*vs.*T (average value and standard deviation) for alloys (a)625, (b)C-22, (c)C-22HS and (d)HYBRID-BC1. Symbols: experimental. Dashed lines: fitting using equation 2.

Table 2 shows the Critical Crevice Temperature (CCT) values obtained from the literature (http://www.haynesintl.com/.) for the tested alloys and those inferred from the present work. CCT values are usually determined after 72 hours of exposure in acidified 6% $FeCl_3$ (ASTM G48 03, 2003). The literature reported CCT values are considerable higher than those obtained in this work. However, the trend of CCT with PREN is the same in both cases. The differences among CCTs are most probably due to the different testing methods and crevicing devices.

Table 2. CCT from literature (http://www.haynesintl.com/) and from the present work.

Alloy	PREN	CCT (literature)	CCT (this work)
625	50.7	40ºC	CCT < 20ºC
C-22	69.9	80ºC	30ºC < CCT < 40ºC
C-22HS	78.8	CCT > 85ºC	30ºC < CCT < 40ºC
HYBRID-BC1	87.6	CCT > 85ºC	50ºC < CCT < 60ºC

Figure 4 shows E_{CO} (average value and standard deviation) obtained using the PD-GS-PD method as a function of chloride concentration for all the tested alloys. As reported previously in the literature, E_{CO} decreased linearly with log [Cl^-] and T for the tested alloys, (Evans et al., 2003; Evans et al., 2005;Rebak, 2005, Dunn et al, 2005).

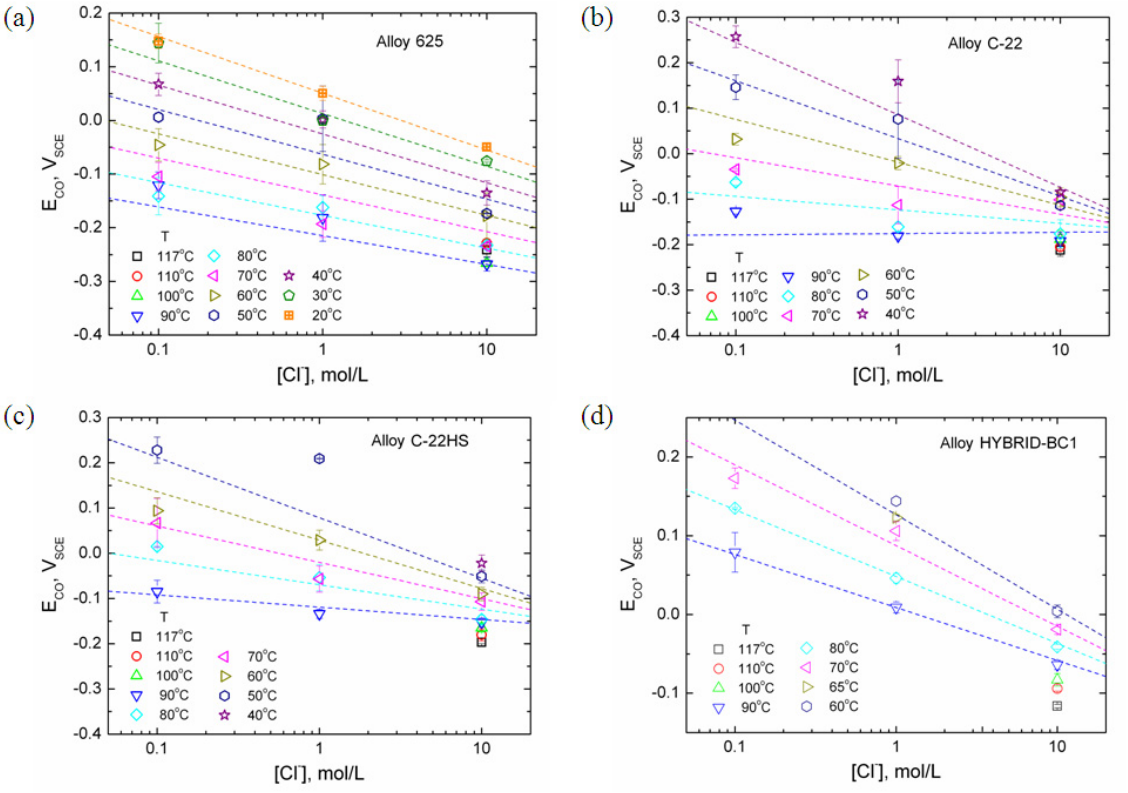

Fig. 4.E_{CO}*vs.*log [Cl-] (average value and standard deviation) for alloys (a)625, (b)C-22, (c)C-22HS and (d)HYBRID-BC1. . Symbols: experimental. Dashed lines: fitting using equation 2.

Several works on the behavior of E_{CO} with temperature and chloride concentration were carried out by different authors (Gordon, 2002; Rebak, 2005; Carranza, 2008). Equation 2 has been used by Dunn (Dunn et al., 2001) to fit E_{CO} of alloy C-22, where a, b, c and d are constants. The same Equation 2 was used in this work to fit to the measured data for each alloy.

$$E_{CO} = (a + bT)\log(Cl^-) + cT + d \quad (2)$$

E_{CO} values for alloy 625 in 10 mol/L chloride concentration and T > 90 ºC were excluded from the fit (saturation of E_{CO} for alloy 625).

Figures 3-4 (described above) show in dash lines the fit obtained using Equation 2 for E_{CO}. There was good agreement between the behavior predicted by Equation 2 and E_{CO} for all the tested alloys. Table 3 shows the values of the constants obtained for each alloy and the R^2 values. The independent term of Equation 2 (d) increased as the value of PREN increased (Table 2). Fitting parameters b and c were similar for all alloys. All the R^2 values from the non-linear fits were above 0.9 which indicated that Equation 2 successfully represented E_{CO} as a function of temperature and chloride concentration for the tested alloys. Values of the fitting parameters for alloy C-22 were similar to those obtained by Dunn (Dunn et al., 2001), except the independent term which was smaller. This difference was attributed to the different testing methods (CPP and PD-GS-PD) along with the difference between

the crevicing devices (PTFE crevice formers give higher E_{CO} values than the PD-GS-PD method (Rincón Ortíz et al., 2010)).

Table 3.Fit parameters of Equation 2.

$E_{CO}=(a+bT)\log[Cl^-]+cT+d$	a (V_{SCE})	b (V/ºC)	c (V/ºC)	d (V_{SCE})	R^2
Alloy 625	-0.121 ±0.015	0.0007 ±0.0002	-0.0038 ±0.0002	0.126 ±0.012	0.901
Alloy C-22	-0.289 ±0.021	0.0032 ±0.0003	-0.0052 ±0.0003	0.294 ±0.019	0.918
Alloy C-22HS	-0.267 ±0.024	0.0027 ±0.0003	-0.0049 ±0.0003	0.326 ±0.023	0.916
Alloy HYBRID-BC1	-0.226 ±0.018	0.0018 ±0.0002	-0.0039 ±0.0002	0.363 ±0.016	0.983

Figure 5 shows SEM images of alloy C-22 after PD-GS-PD tests in different experimental conditions. Crevice corrosion was observed after all the tests shown in Figure 5. There was an increase of the attack with temperature and chloride concentration. On the other way, there was a decrease in the volume of the corrosion products at higher temperatures and chloride concentrations. The morphology of the localized attack was found to be the same for all the tested alloys. The alloy grains were discernible in the attacked areas, especially in the 5 mol/L $CaCl_2$ solutions.

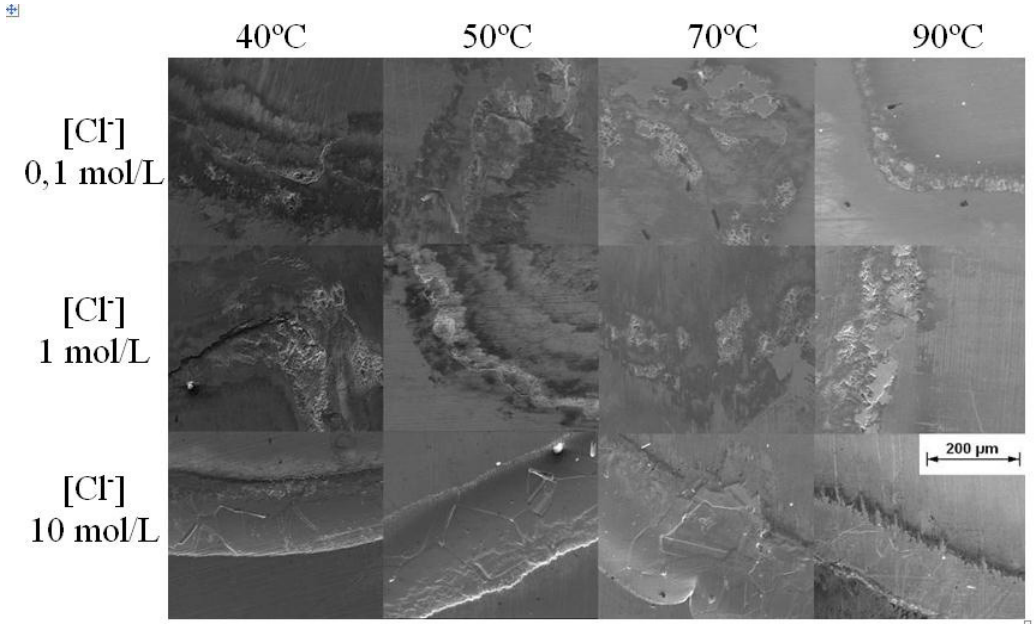

Fig. 5.SEM images of alloy C-22 specimens after PD-GS-PD tests performed in chloride solutions of different concentrations and at different temperatures.

Figure 6a shows 3D graphs for the experimental variation of E_{CO} with temperature and chloride concentration and the fitting results using Equation 2. Figure 6b represents fitting surfaces (meshed surfaces) of all the alloys studied. Crevice corrosion resistance of the alloys increased in the following order: 625 < C-22 < C-22HS < HYBRID-BC1, which is in agreement with their PREN (Table 2). The fitting surfaces of alloys C-22 and C-22HS were quite similar.

Many mechanisms have been proposed to explain pitting corrosion of passive metals (Szklarska-Smialowska, 2005). Galvele has developed a model based on the localized acidification mechanism

(Galvele, 1976; Galvele, 1981, Gravano et al., 1984), which was able to explain several experimental observations (Galvele, 2005). The localized acidification model is able to explain the change in pitting potential with the aggressive anion concentration, and with pH, the influence of weak acids, the existence of repassivation and inhibition potentials, among other experimental observations (Galvele, 2005). The localized acidification model can be extended to crevice corrosion, and through it, obtain a theoretical expression for the variation of crevice corrosion repassivation potential with chloride concentration:

$$E_{CO} = E_0 - \left(\frac{2.3RT}{F}\right) \log[Cl^-] \tag{3}$$

where E_0 is a constant, R is the universal gas constant, T is the absolute temperature and F the Faraday constant.

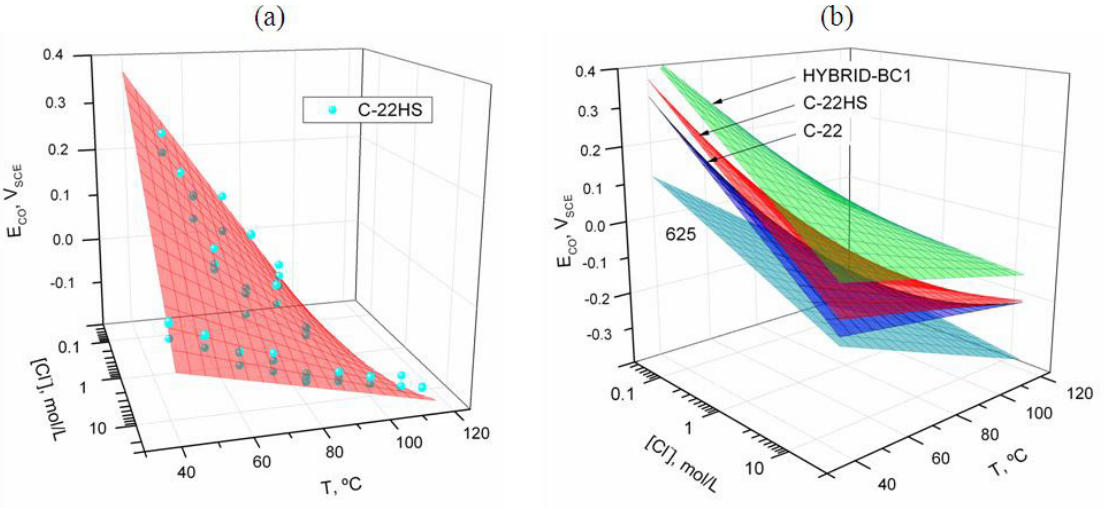

Fig. 6. (a)E_{CO} of alloy C-22HS as a function of temperature and chloride concentration. Symbols: experimental. Mesh: Fitting results using Equation 2 (b) Fitting meshes for the four studied alloys.

Figure 7 shows the derivative of E_{CO} with respect to log $[Cl^-]$ as a function of the temperature along with the theoretical slope obtained by Galvele (from Equation 3). All the alloys showed a decrease in the absolute value of slope as the temperature was increased. Alloy 625 has lower values of $\delta E_{CO}/\delta \log [Cl^-]$ with respect to the other alloys. The estimated error of $\delta E_{CO}/\delta T$, represented as gray bands, increased linearly with temperature. For higher temperatures, all slopes showed similar values. Figure 7 shows that as long as the environmental conditions became more aggressive (increasing T) the absolute values of slopes decreased indicating E_{CO} was less dependent on the environmental variables. Figure 7 shows that as the temperature increases, $\delta E_{CO}/\delta \log [Cl^-]$ approaches the value corresponding to the theoretical slope proposed by Galvele. This theoretical slope considers only the ohmic drop in the solution within the crevice. The differences between experimental and theoretical slopes observed at low temperatures were attributed here to the presence of corrosion products, as those shown in Figure 5, which produced an additional ohmic drop.

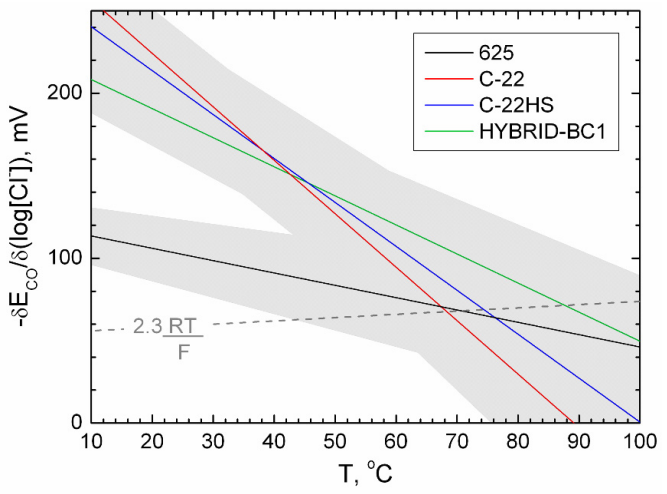

Fig. 7.$\delta E_{CO}/\delta \log [Cl]$ vs.T.

4. Conclusions

- HYBRID-BC1 was the most resistant alloy to chloride-induced crevice corrosion, followed by alloys C-22HS, C-22 and 625. The corrosion resistance of the alloys increased according to their corresponding Pitting Resistance Equivalent Number (PREN).
- The crevice critical temperature (CCT) inferred from the present results are lower than those reported in literature. This was attributed to the different testing methods and/or crevicing devices used.
- The repassivation potential of the tested alloys as a function of temperature and chloride concentration was given by $E_{CO} = (a + b\ T) \log [Cl^-] + c\ T + d$, where a, b, c and d are constants.
- In aggressive environmental conditions (high temperature and chloride concentrations), E_{CO} was independent of T for Alloy 625. This same behavior would be expected for the other alloys for more aggressive conditions than those used in this work. These minimum values are independent of temperature and chloride concentration, and are strong parameters for assessing the localized corrosion susceptibility of the materials in a long term timescale.

Acknowledgements

Financial support from the Agencia Nacional de Promoción Científica y Tecnológica of the Ministerio de Educación, Ciencia y Tecnología from Argentina, and from the Universidad Nacional de San Martín is acknowledged.

References

ASTM G192-08, 2008, -Resistant Alloys Using a Potentiodynamic-Galvanostatic- ASTM Intl., 2008).

ASTM G48-03, 2003, "Standard Test Methods for Pitting and Crevice Corrosion Resistance of Stainless Steels and Rellated Alloys by Use of Ferric Chloride Solutions" Annual Book of ASTM Standards, vol. 03.02 (West Conshohocken, PA: ASTM Intl., 2003), pp. 191-201.

Combrade, P. 2000, Crevice corrosion of metallic materials in Corrosion mechanisms in theory and practice, Second edition, Marcus P. Editor, Marcel Dekker, pp. 349-397.

Cragnolino, G. A., 2001, Long term passive dissolution and localized corrosion of alloy 22, in Proceedings from an international workshop on long-term passive behavior, 19 and 20 July, Arlington, Virginia, editors A. A. Sagüés and C. A. W. Di Bella, USNWTRB, pp. 11-16.

Dunn, D. S., Cragnolino G. A., Y. -M. Pan and O. Pensado, 2001, Corrosion processes affecting the performance of alloy 22 as a high-level radioactive waste container material, in Scientific Basis for Nuclear Waste Management XXIV. K. P. Hart and G. R. Lumpkin, Eds. MRS

Dunn, D. S., Y. –M. Pan, L. Yang and G. A. Cragnolino, 2005, Localized susceptibility of alloy 22 in chloride solutions: part 1 – mill-annealed condition, Corrosion Vol. 61, Nº 11, pp. 1078- 1085.

Evans, K. J., Yilmaz, A., Day, S. D., Wong, L. L. Estill, J. C., Rebak, R. B., 2005, Journal of Metals, p. 56.

Evans, K.J., S.D. Day, G.O. Ilevbare, M.T. Whalen, K.J. King, G.A. Hust, L.A. Wong, J.C. Estill, R.B. Rebak, 2003, "Anodic behavior of Alloy 22 in calcium chloride and in calcium chloride plus calcium nitrate brines", ASME RPV Conference, Cleveland, OH.

Fontana, M., 1986, Corrosion Engineering, Third edition, McGraw-Hill.

Galvele, J. R., 1976, Transport processes and the mechanism of pitting of metals, Journal of The Electrochemical Society, Vol. 123, Nº 4, pp. 464-474,.

Galvele, J. R., 1981, Transport processes in passivity breakdown - II Full hydrolysis of metal ions, Corrosion Science Vol. 21, Nº 8, pp. 551-579.

Galvele, J. R., 2005, Tafel's law in pitting corrosion and crevice corrosion susceptibility, Corrosion Science Vol. 47, pp. 3053–3067.

Galvele, J. R., Duffó, G. S., 2006, Degradación de Materiales. Corrosión. Primera Edición, Jorge Baudino Ediciones, Instituto Sabato, Buenos Aires.

Gras, J. M., 2002, C. R. Physique 3, p. 891.

Gordon, G. M., 2002, Corrosion, Vol. 58 Nº 10, pp. 811-825.

Gravano, S. M. andGalvele J. R.,1984, Transport processes in passivity breakdown - III Full hydrolysis plus ion migration plus buffers, Corrosion Science Vol. 24, Nº 6, pp. 517-534.

http://www.haynesintl.com/. (Consulted on March, 2013)

MacDougall, B. R., 2001, Reply to the questions on long-term passivity and localized corrosion of alloy 22, in Proceedings from an international workshop on long-term passive behavior, 19 and 20 July, Arlington, Virginia, editors A. A. Sagüés and C. A. W. Di Bella, USNWTRB, pp. 49-54.

Mishra, A. K., Frankel, G. S., 2008, Corrosion, Vol. 64, Nº 11, p. 836.

Rebak, R. B., 2000, Materials science and technology. A comprehensive treatment. Corrosion and environmental degradation, Vol. II, pp. 69-111, Schuntze, M., Editor, Wiley, VCH.

Rebak, R. B. 2005, "Factors affecting the crevice corrosion susceptibility of Alloy 22", Paper Nº05610, Corrosion/05, NACE Intl., Houston, TX, 2005

Rincón Ortíz, M., Rodríguez, M. A., Carranza, R. M., Rebak, R. B., 2010, Corrosion, Vol. 66, Nº 10.

Szklarska-Smialowska, Z., 2005 Pitting and Crevice Corrosion, NACE International.

Warrendale, PA. Symposium Proceedings, Vol. 663.

Whiterspoon, P. A., Bodvarsson, G. S., 2001, Geological Challenges in Radioactive Waste Isolation, Third Worldwide Review, University of California, Berkeley, CA, USA.Deal, B., Grove, A., 1965.

Yucca Mountain Science and Engineering Report, 2001, U. S. Department of Energy, Office of Civilian Radioactive Waste Management, DOE/RW-0539, Las Vegas, NV.

Zadorozne, N. S., Giordano, C. M., Rodríguez, M. A., Carranza, R. M. &Rebak, R. B., 2012, Crevice corrosion kinetics of nickel alloys bearing chromium and molybdenum. ElectrochimicaActa 76, 94–101.